IFSCC 2025 full paper (FSCC2025-1787)

"Permeation of small molecules through biological and synthetic skin models using an organ-on-chip platform under controlled dosing conditions."

Massimo Alberti [1], Sebastien Teissier [1]

[1] REVIVO BioSystems Pte. Ltd.

1. Introduction

Transdermal drug delivery offers a non-invasive route that bypasses the gastrointestinal tract and first-pass metabolism. However, its success depends on the ability of compounds to permeate the stratum corneum (SC), the skin's outer barrier.

Pre-clinical permeation studies are essential to assess drug diffusion across skin layers using in vitro and in vivo models like diffusion cells, reconstructed skins, and simulations [1,2]. These studies ensure that formulations achieve therapeutic levels while minimizing adverse effects [3].

1.1 Skin Simulants

1.1.1 Native Human Skin

Skin simulants play a crucial role in permeation testing, each offering unique advantages and limitations. Native human skin is considered the gold standard due to its biological properties, but its use is hindered by donor variability and limited availability, with freezing further reducing viability [4,5]. Porcine skin, structurally similar to human skin, provides a cost-effective alternative, but inter-animal variability and physiological differences limit its translational relevance.

Synthetic membranes offer consistent data due to their uniform structure [6,7] but lack the biological complexity of human skin. In contrast, reconstructed skin models, or Human Skin Equivalents (HSEs), mimic human skin structure and disease states [8–14], but their lack of appendages (such as glands and follicles) limits their ability to model appendageal pathways [15–18].

Selecting the appropriate skin simulant depends on the study's requirements, balancing biological relevance with practical considerations in controlled dosing conditions on organ-on-chip platforms.

1.2 Permeation Apparatuses

Permeation apparatuses are essential for studying the transport of small molecules through biological and synthetic skin models. Among the most widely used systems are static diffusion cells, such as Franz cells [19]. These devices consist of a static receptor chamber located beneath a membrane, offering controlled experimental conditions. However, they often face challenges in maintaining sink conditions, particularly when testing low-solubility drugs. Additionally, they require relatively large skin samples, and manual handling can introduce variability, affecting reproducibility.

Flow-through diffusion cells offer an alternative by continuously flushing the receptor solution, thereby mimicking physiological flow and facilitating the removal of metabolites. This dynamic approach makes them valuable for metabolism studies. However, the flow rates used in these setups may exceed physiological norms [20–22], raising concerns about the relevance of the results for in vivo conditions.

To overcome the limitations of traditional setups, miniaturized microfluidic systems have emerged. These devices use significantly less drug and sample material while providing precise control over laminar flow, enhancing reproducibility. Moreover, they enable high-throughput analysis, making them particularly suitable for screening studies [6,9,23–28]. Consequently, microfluidic systems represent a modern and efficient approach to studying permeation under controlled conditions.

1.3 Caffeine Permeation

This study compared different skin simulants and assessed caffeine permeation using an automated microfluidic platform across various skin simulants. Caffeine is common in cosmetics (up to 5%) for its antioxidant, microcirculation, and skin barrier benefits [29–32], but its hydrophilicity limits skin permeation [2]. The automated microfluidic system offers precise, reproducible testing with reduced manual handling. Its adaptability for finite and infinite doses across different skin models makes it a valuable tool for transdermal delivery research.

2. Materials and Methods

2.1 Automated Microfluidic Permeation Platform

Caffeine permeation tests were performed on a our automated fraction collector fitted with four REV*ex* microfluidic chips (REVIVO BioSystems, Singapore), based on the design reported in [27]. Each REV*ex* chip contains three independent microfluidic diffusion units accommodating 8 mm diameter skin simulants and a dosing bar with a diffusion area of 0.2 cm².

Effluent receptor vehicle continuously dripped from each unit into wells of moving 96-well plates, with the flow rate maintained by an external peristaltic pump. Fraction collection was automated, ensuring precise timing and temperature control throughout the experiment.

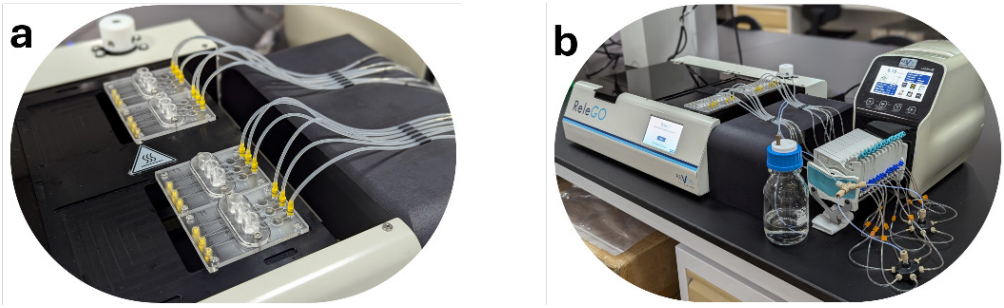

Figure 1. Setup of the caffeine and salicylic acid permeation studies on the microfluidic permeation array through 8 skin simulants. (a) Four REV*ex* microfluidic permeation arrays are connected to the peristaltic pump and placed onto the heating bridge of the Rele*GO*. (b) Permeation setup consisting of the Rele*GO* fraction collector, a peristaltic pump, tubing and receiver solution bottle.

2.2 Chemicals and Formulations

Caffeine and ethanol were obtained from Sigma-Aldrich (Singapore), and PBS from GE Healthcare (USA).

- **Infinite dose**: 13.5 mg/mL caffeine solution prepared in PBS, stirred overnight.
- **Finite dose**: 2.0 mg/mL caffeine solution prepared in 50% ethanol and 50% DI water.

2.3 Preparation of Skin Simulants

- **Reconstructed skins** (T-SKIN, RHE/L, EpiDerm-X) were prepared according to manufacturer protocols, cut into 8 mm discs, and mounted on REVex chips.
- **Porcine skin** was sourced from pig ears, dermatomed to 0.5 mm, and punched into 8 mm discs.
- **Human abdominal skin** (400–700 µm thick) was sourced from Biopredic International (France).
- **Synthetic membranes** (Silicone, Strat-M) were cut to size and mounted accordingly.

All biological samples were PBS-rinsed overnight before dosing.

2.4 Topical Application and Permeation Tests

- **Infinite dose**: 240 µL of 13.5 mg/mL caffeine solution applied per dosing chamber.
- **Finite dose**: 10 µL of 2 mg/mL caffeine solution applied per chamber.

In all the studies, the receiver vehicle was PBS. The permeation tests ran for 20 hours at 4 µL/min flow rate, with 1-hour fraction collection intervals (240 µL collected per interval).

2.5 Analytical Procedure

UV spectrophotometry (Spark, Tecan, Switzerland) was used to quantify caffeine at 272 nm according to the method described in [27], with the the limits of detection in the range of 0.03-0.21 µg/mL and limits of quantification in the range of 0.11-0.69 µg/mL. For infinite doses, steady-state flux (J_{ss}) and lag time (t_{lag}) were derived from the cumulative permeation profile.

The apparent permeability coefficient (k_p) was calculated per Fick's law. For finite doses, maximum flux (J_{max}) and peak time (t_{peak}) were extracted from the flux profiles.

2.6 Mass Balance

After permeation, residual donor solution was collected and receptor compartments were flushed with PBS. Skin simulants were submerged in PBS for 24 hours to quantify retained caffeine.

3. Results

3.1 Infinite Doses

The receptor cumulative amount profiles, permeability coefficients (k_p), steady-state fluxes (J_{ss}), and lag times (t_{lag}) for caffeine permeation under infinite dose conditions are shown in Figure 2 and Table 1.

Among reconstructed skin models, MatTek's EpiDerm EPI-X exhibited the highest barrier, with a k_p about 10 times lower and t_{lag} of 2.0 h compared to EPISKIN's T-SKIN and RHE. T-SKIN showed higher permeability than RHE but had the lowest variability (CV%). Permeability coefficients for reconstructed skins were approximately two orders of magnitude higher than those of *ex vivo* human and porcine skins (Figure 2c). Native human skin had a k_p of 0.16×10^{-3} cm/h, about 3.1 times lower than porcine skin.

Silicone membranes demonstrated thickness-dependent behavior, with 0.5 mm thick silicone membranes and 0.25 mm thick silicone membranes matching human skin permeability coefficient and porcine skin permeability coefficient, respectively. Strat-M membranes showed significantly higher permeability than native skin, suggesting a poor correlation for caffeine infinite dose studies.

Despite significant caffeine uptake in reconstructed tissues (up to 68%), steady-state flux conditions were maintained across all models during the 20h study.

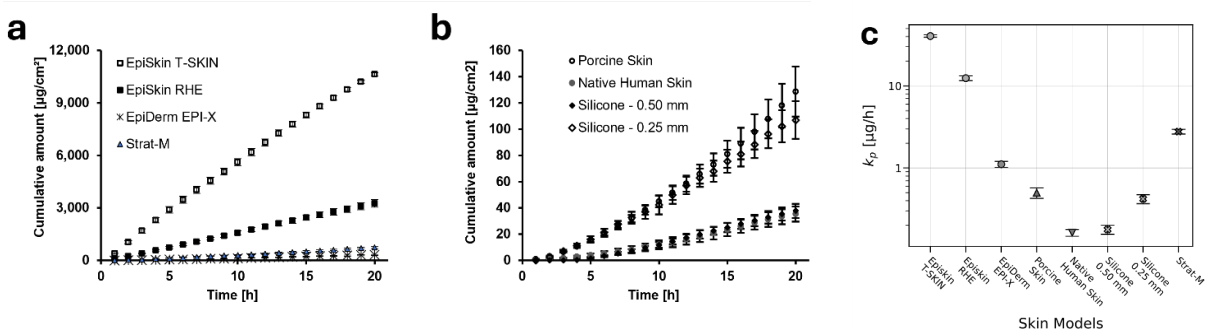

Figure 2: Comparison of eight different skin simulants' barrier function for an infinite dose of caffeine in PBS (16.5 mg/cm^2). (a) & (b) Cumulative amount profiles of caffeine permeation through the eight skin simulants, with higher caffeine permeability (a) and lower caffeine permeability (b). (c) Caffeine permeability coefficients.

Table 1. Mean and standard deviations of the permeation parameters and recovered permeant for an infinite dose of caffeine through different skin simulants (Donor concentration: 13.5 mg/mL; Dose: 16.5 mg/cm^2).

Skin simulants	# of replicates	Steady state flux [µg/cm^2 h^{-1}]	Lag time [h]	k_p [×10^{-3} cm h^{-1}]	Permeant penetrated [%]	Permeant uptake [%]
T-SKIN (EPISKIN)	4	584.4 ± 19.87	0.2 ± 0.12	40.5 ± 1.38	60.2 ± 0.43	68.3 ± 0.66
RHE (EPISKIN)	6	168.7 ± 11.14	0.6 ± 0.14	12.4 ± 0.82	19.7 ± 1.32	22.0 ± 1.43
EPI-X (MatTek Corporation)	3	17.0 ± 1.45	2.0 ± 0.06	1.1 ± 0.09	1.7 ± 0.15	2.5 ± 0.08
Porcine Skin	4	6.6 ± 0.95	3.0 ± 0.40	0.5 ± 0.07	0.8 ± 0.12	1.4 ± 0.1
Native Human Skin	4	2.4 ± 0.23	5.4 ± 1.16	0.16 ± 0.015	0.2 ± 0.03	0.3 ± 0.04
Silicone – 0.5 mm	6	2.5 ± 0.32	4.9 ± 0.19	0.18 ± 0.023	0.2 ± 0.03	0.4 ± 0.04
Silicone – 0.25 mm	6	5.9 ± 0.74	2.3 ± 0.33	0.42 ± 0.053	0.6 ± 0.1	0.8 ± 0.08
Strat-M	6	39.0 ± 2.63	1.6 ± 0.05	2.8 ± 0.19	4.3 ± 0.29	5.5 ± 0.48

3.1.2 Finite Doses

Flux profiles, cumulative amounts, and permeation parameters for finite doses of caffeine are presented in Figure 3 and Table 2.

T-SKIN and RHE showed one order of magnitude higher maximum flux (J_{max}) than porcine and human skins and earlier peak times (~2 h). EPI-X exhibited J_{max} values about twice those observed in porcine skin but maintained similar t_{peak} (~5–6 h). Native human skin displayed the lowest J_{max} and latest t_{peak} (~8 h). Synthetic membranes (silicone, Strat-M) did not show measurable caffeine permeation.

Mass balances revealed high uptake (>70%) in reconstructed skins compared to <50% in *ex vivo* skins. Strat-M membranes retained caffeine strongly, requiring heat treatment to release it fully, unlike other models.

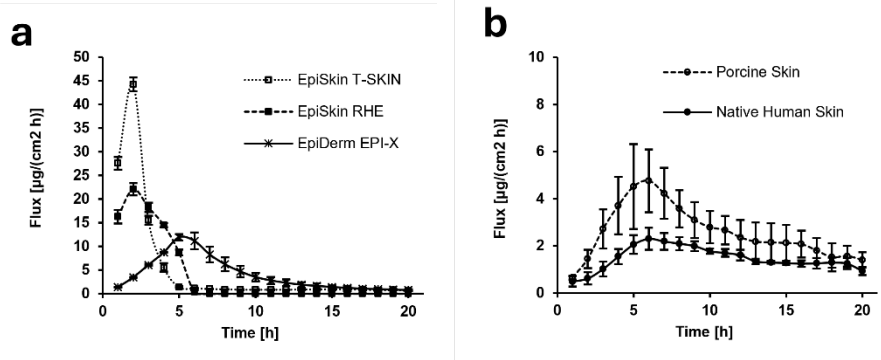

Figure 2: Comparison of five different skin simulants' barrier function for a finite dose of caffeine (0.1 mg/cm^2) in Ethanol:DI water 1:1. (a) and (b) Flux profiles of caffeine permeation.

Table 2. Mean and standard deviations of the permeation parameters and recovered permeant for a finite dose of caffeine (0.1 mg/cm^2) in Ethanol:DI water 1:1 through different skin models (Donor concentration: 2.0 mg/mL; Applied volume: 10 µL).

Skin simulants	# of replicates	Maximum flux [µg/cm^2 h^{-1}]	Peak Time [h]	Permeant penetrated [%]	Permeant uptake [%]
T-SKIN (EPISKIN)	4	44.2 ± 1.48	2.0 ± 0	96.2 ± 2.33	99.7 ± 2.06
RHE (EPISKIN)	4	22.1 ± 1.3	2.0 ± 0	78.1 ± 2.8	79.6 ± 2.89
EPI-X (MatTek Corporation)	3	11.9 ± 0.72	5.7 ± 0.47	71.6 ± 10.3	78.7 ± 10.74
Porcine Skin	4	5.8 ± 2.55	5.1 ± 1.17	42.3 ± 11.0	48.2 ± 12.85
Native Human Skin	3	2.4 ± 0.41	8.0 ± 1.63	24.6 ± 2.87	28.8 ± 1.26
Silicone – 0.5 mm	4	N.A.	N.A.	N.A.	7.5 ± 1.45
Silicone – 0.25 mm	4	N.A.	N.A.	N.A.	12.0 ± 4.35
Strat-M	6	N.A.	N.A.	N.A.	87.2 ± 4.12

4. Discussion

4.1 Infinite Dose Caffeine Permeation

The permeability differences among skin simulants reflected their structural characteristics. EPI-X provided a closer approximation to human skin barrier function compared to other reconstructed tissues.Native human skin's results aligned with literature [5,33,34], confirming the reliability of the microfluidic platform. Silicone membranes successfully mimicked skin resistance depending on thickness, with 0.5 mm membranes corresponding well to human skin. Strat-M membranes, however, were not suitable due to their high permeability for caffeine. The unexpected strong retention of caffeine in Strat-M also highlights the risk of using some types of synthetic membranes for caffeine-related permeation studies without careful validation, especially in ethanol-containing formulations. Further investigations into the chemical interactions between Strat-M and caffeine are warranted.

Dynamic flow conditions in the microfluidic setup preserved sink conditions, enabling pseudo-infinite dosing across all skin models even with high uptake.

4.2 Finite Dose Caffeine Permeation

Finite dose experiments confirmed that reconstructed skin equivalents offered lower barrier properties than native tissues. Human skin consistently provided the most restrictive permeation profile, followed by porcine skin. Good agreement was found with previous caffeine permeation studies [35–37]. The failure to detect caffeine permeation through synthetic membranes in finite doses studies points to sensitivity limitations of the analytical method and strong caffeine binding to Strat-M membranes. Future studies could improve finite dose analysis by increasing donor concentration, refining ethanol concentration, and using more sensitive detection methods.

5. Conclusion

This study utilized an automated microfluidic permeation platform paired with REV*ex* chips to investigate the permeation of caffeine through eight different skin simulants. The REV*ex* chip,

featuring three independent flow-through diffusion units, enabled dynamic testing under physiologically relevant conditions across *in vitro*, *ex vivo*, and synthetic models.

Under infinite dose conditions, reconstructed skin models exhibited permeability coefficients (k_p) one to two orders of magnitude higher than porcine and human skins. Notably, silicone membranes approximated the permeability of native skins, indicating their suitability as substitutes in caffeine studies. Under finite dose conditions, reconstructed skin equivalents showed the highest flux, while synthetic membranes failed to permit any detectable caffeine permeation. Among all models, EPISKIN T-SKIN demonstrated the lowest variability, highlighting the stabilizing role of the dermal layer in epidermal development and reproducibility. The results obtained align well with previously published caffeine permeation data, validating both the biological models and experimental platform.

The microfluidic system's automated operation, low flow rate precision, and continuous sink condition maintenance significantly enhance the sensitivity and reproducibility of permeation assays. These features are especially valuable when working with low-flux compounds such as caffeine.

In summary, this automated microfluidic platform proves to be a robust, efficient, and versatile tool for conducting infinite and finite dose caffeine permeation studies, offering reliable data under controlled, physiologically relevant conditions, and supporting its application in transdermal drug delivery research.

1 References

[1] P.J.C. da Costa, A.I.M. de Jesus, I.F.M. de Almeida, Tissue-based in vitro and ex vivo models for dermal permeability studies, in: Concepts Model. Drug Permeability Stud., Elsevier, 2024: pp. 479–500. https://doi.org/10.1016/B978-0-443-15510-9.00015-3.

[2] R. Reyes, M.S. Abou-Dahech, N. (Gina) Nguyen, A. Smith, R.C. Devore Homan, I.T. Schiefer, M. Chandler, G. Baki, Skin penetration of caffeine from commercial eye creams and eye creams designed and optimized based on Hansen solubility parameters, Int. J. Pharm. 639 (2023) 122973. https://doi.org/10.1016/j.ijpharm.2023.122973.

[3] E. Abd, S. Yousuf, M. Pastore, K. Telaprolu, Y. Mohammed, S. Namjoshi, J. Grice, M. Roberts, Skin models for the testing of transdermal drugs, Clin. Pharmacol. Adv. Appl. Volume 8 (2016) 163–176. https://doi.org/10.2147/CPAA.S64788.

[4] L.A. AHLSTROM, S.E. CROSS, P.C. MILLS, The effects of freezing skin on transdermal drug penetration kinetics, J. Vet. Pharmacol. Ther. 30 (2007) 456–463. https://doi.org/10.1111/j.1365-2885.2007.00879.x.

[5] A.M. Barbero, H.F. Frasch, Effect of Frozen Human Epidermis Storage Duration and Cryoprotectant on Barrier Function Using Two Model Compounds, Skin Pharmacol. Physiol. 29 (2016) 31–40. https://doi.org/10.1159/000441038.

[6] C. Provin, A. Nicolas, S. Grégoire, T. Fujii, A Microfluidic Diffusion Cell for Fast and Easy Percutaneous Absorption Assays, Pharm. Res. 32 (2015) 2704–2712. https://doi.org/10.1007/s11095-015-1654-x.

[7] H. Kichou, F. Bonnier, Y. Dancik, J. Bakar, R. Michael-Jubeli, A.C. Caritá, X. Perse, M. Soucé, L. Rapetti, A. Tfayli, I. Chourpa, E. Munnier, Strat-M® positioning for skin

permeation studies: A comparative study including EpiSkin® RHE, and human skin, Int. J. Pharm. 647 (2023) 123488. https://doi.org/10.1016/j.ijpharm.2023.123488.

[8] C.A. Brohem, L.B. da Silva Cardeal, M. Tiago, M.S. Soengas, S.B. de Moraes Barros, S.S. Maria-Engler, Artificial skin in perspective: concepts and applications, Pigment Cell Melanoma Res. 24 (2011) 35–50. https://doi.org/10.1111/j.1755-148X.2010.00786.x.

[9] G. Sriram, M. Alberti, Y. Dancik, B. Wu, R. Wu, Z. Feng, S. Ramasamy, P.L. Bigliardi, M. Bigliardi-Qi, Z. Wang, Full-thickness human skin-on-chip with enhanced epidermal morphogenesis and barrier function, Mater. Today 21 (2018) 326–340. https://doi.org/10.1016/j.mattod.2017.11.002.

[10] E. Michielon, M. López González, D.A. Stolk, J.G.C. Stolwijk, S. Roffel, T. Waaijman, S.M. Lougheed, T.D. de Gruijl, S. Gibbs, A Reconstructed Human Melanoma-in-Skin Model to Study Immune Modulatory and Angiogenic Mechanisms Facilitating Initial Melanoma Growth and Invasion, Cancers (Basel). 15 (2023) 2849. https://doi.org/10.3390/cancers15102849.

[11] E.S.P. Aranha, L. de S. Mendonça, B. de L. Almeida, E.L. da Silva, F.P. Mesquita, E.S. Lima, A.P.N.N. Alves, M.E.A. de Moraes, R.C. Montenegro, M.C. de Vasconcellos, Three dimensional reconstruction of skin with melanoma: A model for study of invasion in vitro, Toxicol. Vitr. 99 (2024) 105883. https://doi.org/10.1016/j.tiv.2024.105883.

[12] M.S. Shutova, J. Borowczyk, B. Russo, S. Sellami, J. Drukala, M. Wolnicki, N.C. Brembilla, G. Kaya, A.I. Ivanov, W.-H. Boehncke, Inflammation modulates intercellular adhesion and mechanotransduction in human epidermis via ROCK2, IScience 26 (2023) 106195. https://doi.org/10.1016/j.isci.2023.106195.

[13] E. Desmet, A. Ramadhas, J. Lambert, M. Van Gele, In vitro psoriasis models with focus on reconstructed skin models as promising tools in psoriasis research, Exp. Biol. Med. 242 (2017) 1158–1169. https://doi.org/10.1177/1535370217710637.

[14] M. Ahn, W.-W. Cho, W. Park, J.-S. Lee, M.-J. Choi, Q. Gao, G. Gao, D.-W. Cho, B.S. Kim, 3D biofabrication of diseased human skin models in vitro, Biomater. Res. 27 (2023) 1–13. https://doi.org/10.1186/s40824-023-00415-5.

[15] N. Otberg, A. Patzelt, U. Rasulev, T. Hagemeister, M. Linscheid, R. Sinkgraven, W. Sterry, J. Lademann, The role of hair follicles in the percutaneous absorption of caffeine, Br. J. Clin. Pharmacol. 65 (2008) 488–492. https://doi.org/10.1111/j.1365-2125.2007.03065.x.

[16] A. Pappalardo, A. Cespedes, H.L. Vu, H.E. Abaci, Advances in skin-on-a-chip and skin tissue engineering, in: Princ. Hum. Organs-on-Chips, Elsevier, 2023: pp. 123–166. https://doi.org/10.1016/B978-0-12-823536-2.00005-5.

[17] H.E. Abaci, K. Gledhill, Z. Guo, A.M. Christiano, M.L. Shuler, Pumpless microfluidic platform for drug testing on human skin equivalents, Lab Chip 15 (2015) 882–888. https://doi.org/10.1039/C4LC00999A.

[18] K. Schimek, H.-H. Hsu, M. Boehme, J. Kornet, U. Marx, R. Lauster, R. Pörtner, G. Lindner, Bioengineering of a Full-Thickness Skin Equivalent in a 96-Well Insert Format for Substance Permeation Studies and Organ-On-A-Chip Applications, Bioengineering 5 (2018) 43. https://doi.org/10.3390/bioengineering5020043.

[19] S.-F. Ng, J.J. Rouse, F.D. Sanderson, V. Meidan, G.M. Eccleston, Validation of a Static Franz Diffusion Cell System for In Vitro Permeation Studies, AAPS PharmSciTech 11 (2010) 1432–1441. https://doi.org/10.1208/s12249-010-9522-9.

[20] D.J. Harrison, K. Knutson, Accurate Determination of Skin Flux from Flow-Through Diffusion Cell Data, Pharm. Res. An Off. J. Am. Assoc. Pharm. Sci. 12 (1995) 2003–2011. https://doi.org/10.1023/A:1016216611809.

[21] W.G. Reifenrath, B. Lee, D.R. Wilson, T.S. Spencer, A comparison of in vitro skin-penetration cells, J. Pharm. Sci. 83 (1994) 1229–1233. https://doi.org/10.1002/jps.2600830908.

[22] M. Córdoba-Díaz, M. Nova, B. Elorza, D. Córdoba-Díaz, J.. Chantres, M. Córdoba-Borrego, Validation protocol of an automated in-line flow-through diffusion equipment for in vitro permeation studies, J. Control. Release 69 (2000) 357–367. https://doi.org/10.1016/S0168-3659(00)00306-0.

[23] D. Ding, J. Pan, S.H. Yeo, V. Wagholikar, S.H. Lim, C. Wu, J.Y.H. Fuh, L. Kang, A miniaturized device for biomembrane permeation analysis, Mater. Sci. Eng. C 103 (2019) 109772. https://doi.org/10.1016/j.msec.2019.109772.

[24] C.S. Mah, J. Singh Kochhar, P.S. Ong, L. Kang, A miniaturized flow-through cell to evaluate skin permeation of endoxifen, Int. J. Pharm. 441 (2013) 433–440. https://doi.org/10.1016/j.ijpharm.2012.11.011.

[25] B. Lukács, Á. Bajza, D. Kocsis, A. Csorba, I. Antal, K. Iván, A.J. Laki, F. Erdő, Skin-on-a-Chip Device for Ex Vivo Monitoring of Transdermal Delivery of Drugs—Design, Fabrication, and Testing, Pharmaceutics 11 (2019) 445. https://doi.org/10.3390/pharmaceutics11090445.

[26] C. Schmidt, J. Markus, H. Kandarova, J. Wiest, Tissue-on-a-Chip: Microphysiometry With Human 3D Models on Transwell Inserts, Front. Bioeng. Biotechnol. 8 (2020) 1–8. https://doi.org/10.3389/fbioe.2020.00760.

[27] M. Alberti, Y. Dancik, G. Sriram, B. Wu, Y.L. Teo, Z. Feng, M. Bigliardi-Qi, R.G. Wu, Z.P. Wang, P.L. Bigliardi, Multi-chamber microfluidic platform for high-precision skin permeation testing, Lab Chip 17 (2017) 1625–1634. https://doi.org/10.1039/C6LC01574C.

[28] P. V. Mohanan, Microfluidics and Multi Organs on Chip, Springer Nature Singapore, Singapore, 2022. https://doi.org/10.1007/978-981-19-1379-2.

[29] J.M. Brandner, M.J. Behne, B. Huesing, I. Moll, Caffeine improves barrier function in male skin, Int. J. Cosmet. Sci. 28 (2006) 343–347. https://doi.org/10.1111/j.1467-2494.2006.00346.x.

[30] A. Herman, A.P. Herman, Caffeine's Mechanisms of Action and Its Cosmetic Use, Skin Pharmacol. Physiol. 26 (2013) 8–14. https://doi.org/10.1159/000343174.

[31] J. Jagdeo, N. Brody, Complementary antioxidant function of caffeine and green tea polyphenols in normal human skin fibroblasts., J. Drugs Dermatol. 10 (2011) 753–61. http://www.ncbi.nlm.nih.gov/pubmed/21720657.

[32] J.I. Silverberg, M. Patel, N. Brody, J. Jagdeo, Caffeine protects human skin fibroblasts from acute reactive oxygen species-induced necrosis., J. Drugs Dermatol. 11 (2012)

1342–6. http://www.ncbi.nlm.nih.gov/pubmed/23135086.

[33] L. Cole, C. Heard, Skin permeation enhancement potential of Aloe Vera and a proposed mechanism of action based upon size exclusion and pull effect, Int. J. Pharm. 333 (2007) 10–16. https://doi.org/10.1016/j.ijpharm.2006.09.047.

[34] M. DIAS, J. HADGRAFT, M. LANE, Influence of membrane–solvent–solute interactions on solute permeation in skin, Int. J. Pharm. 340 (2007) 65–70. https://doi.org/10.1016/j.ijpharm.2007.03.030.

[35] F. Muhammad, J.E. Riviere, Differential effects of some natural compounds on the transdermal absorption and penetration of caffeine and salicylic acid, Int. J. Pharm. 483 (2015) 151–157. https://doi.org/10.1016/j.ijpharm.2015.02.029.

[36] D. SOUTHWELL, B. BARRY, Penetration enhancement in human skin; effect of 2-pyrrolidone, dimethylformamide and increased hydration on finite dose permeation of aspirin and caffeine, Int. J. Pharm. 22 (1984) 291–298. https://doi.org/10.1016/0378-5173(84)90029-2.

[37] J.J.M. van de Sandt, J.A. van Burgsteden, S. Cage, P.L. Carmichael, I. Dick, S. Kenyon, G. Korinth, F. Larese, J.C. Limasset, W.J.M. Maas, L. Montomoli, J.B. Nielsen, J.-P. Payan, E. Robinson, P. Sartorelli, K.H. Schaller, S.C. Wilkinson, F.M. Williams, In vitro predictions of skin absorption of caffeine, testosterone, and benzoic acid: a multi-centre comparison study, Regul. Toxicol. Pharmacol. 39 (2004) 271–281. https://doi.org/10.1016/j.yrtph.2004.02.004.